Inband and out-of-band performance evaluation of downlink CF-mMIMO-OFDM under low-resolution DACs

Antoine Durant, Rafik Zayani, David Demmer

Inband and Out-of-Band Performance Evaluation of Downlink CF-mMIMO-OFDM under low-resolution DACs

Antoine Durant, Rafik Zayani, Asma Mabrouk, David Demmer
CEA-Leti, Univ. Grenoble Alpes, F-38000 Grenoble, France
{antoine.durant, rafik.zayani, asma.mabrouk, david.demmer}@cea.fr

***Abstract*—Cell-free massive MIMO (CF-mMIMO) technology has proved to offer significant gains in terms of spectral efficiency (SE). However, it can be economically attractive only when adopting low cost and energy-efficient hardware. This hardware includes components such as low-resolution digital-to-analog converters (DACs), and causes signal distortions called hardware impairments (HWI). In this paper, first, we propose an analytical characterization for low-resolution DAC where the exact behavior can be described, allowing to shine a new light on DAC-induced distortions. Based on the well-known Bussgang decomposition, we derive for a known signal distribution through closed-form expressions based on the integer and fractional resolution separately for downlink SE performance of orthogonal frequency multiplexing (OFDM) based CF-mMIMO. Moreover, we propose a new CF-mMIMO-specific framework to observe the out-of-band (OOB) radiations on potential victim users. We point out that OOB radiations is less of a problem in multi-user CF-mMIMO, where the total OOB radiated power is sufficiently low to respect any standard mask. Meanwhile, inband distortions represent a serious problem that have to be tackled.**

***Index Terms*—B5G/6G, multi-user MIMO, distributed MIMO, massive MIMO, local precoding**

I. Introduction

In the pursuit of higher data rate and more robust and consistent quality of service (QoS) from wireless networks that are required for 6G, a paradigm shift in network design philosophy seems unavoidable. Distributed massive MIMO system coined CF-mMIMO systems where the antennas are spatially spread among several access points (APs). It allows to alleviate two inherent problems of cellular network : inter-cell interference thanks to a cooperative transmission scheme, and lack of macro diversity which can cause a partial or total shadowing or an increased AP to user equipment (UE) distance [1]. While providing significantly improved performance in most scenarios, early practical implementation studies considering a finite capacity of the fronthaul link shown that it would get too congested if all APs were to fully cooperate and transmit their local channel state information (CSI) [2]. For this reasons, CF-mMIMO transmission filters are computed using only the local CSI, which is an approach known as local precoding [3] which provides limited performance degradation with regards to the fully cooperative schemes [4].

The second limiting factor regarding CF-mMIMO network is due to the expected use of easy to deploy, cheap, and low energy APs for economical viability. Such material is available at the cost of higher hardware-induced signal distortions in the radiofrequency (RF) chains [5]. Although PA impairment has been thoroughly studied in the literature, DAC suffer from a lack of a pertinent characterization. More specifically, DACs have been often modelled using the additive quantization noise model (AQNM) [6] with standard coefficients independent of the input distribution [7], [8]. While it provides a satisfying empirical estimation of the impact of DAC-induced HWI on the system performance, we stress that developing a deterministic model for the DAC based on its inherent properties and the input signal is key to enable future hardware-aware precoding solutions. Furthermore, when it comes to non-linearities, studies mainly focus on in-band effects and out-of-band behavior has only lately been investigated [9]. While the commonly used adjacent-channel leakage ratio (ACLR) is an indicator of interest to evaluate the undesired out-of-band emissions, it seems more relevant to estimate such power at the receiver (the UEs) in distributed systems such as CF-mMIMO. Indeed, because of cooperative transmissions and due to the APs being spread among several locations, a new framework is required. Consequently, in this work, we focus on investigating the non-linear distortions brought by quantified DACs on an OFDM-based CF-mMIMO system.

A. Related works

Modeling studies on quantified DAC have been carried for finite resolution neural network designed to reduce computational complexity and improve energy efficiency [10], but equivalent approach have never been applied in CF-mMIMO literature. Furthermore, signal processing algorithms aimed at reducing the HWI and based on realistic component behavior have been developed for the PA-induced distortions and provides encouraging results [11]. Another lacking point resides in the analysis of the impact of non-linearities being limited to the in-band performance in the CF-mMIMO literature. In [9], a KPI called out-of-band (OOB) radiation is used to quantify the amount of power experienced at the position of the UEs on an adjacent channel, but the framework is developed only for co-localized mMIMO and doesn't account for the contribution of multiple APs.

B. Contributions

In this work, we propose three original contributions. They are as follows :

- Contrary to work in [6] that considers an additive noise model for low resolution DAC, we introduce an analytical characterization of fixed-point quantization based DACs.

We express the characteristics of the DAC with regards to the fixed-point resolution of the fractional and the integer part components, and provide a novel analytic derivation of the Bussgang coefficients.
- We develop analytical expressions for downlink (DL) SE performance of partial-zero forcing (PZF) precoder [3] based CF-mMIMO-OFDM under low-resolution DACs.
- We develop a framework for the analysis of the out-of-band radiation caused by the non-linearities induced by low-resolution DACs which is suitable to the peculiarities of CF-mMIMO, something that has never been studied in the open literature.

II. OFDM-BASED DOWNLINK CF-MMIMO UNDER HWI

A. Network & Channel model

We consider a CF-mMIMO system consisting of L APs equipped by M isotropic antennas to serve K single-antenna UEs within a specific geographic area. The APs are placed on the outer edge of a square area and the UEs are randomly distributed within the surface. Our system is operating in time-division duplexing (TDD). We assume perfect channel reciprocity between the uplink and downlink. In addition, based on OFDM modulation, we consider a flat frequency response over the frequency slot allocated to any sub-carrier n. The total number of sub-carrier is denoted by N and the system bandwidth by B. We consider a block-fading channel model where a channel is considered static for a duration called the coherence interval. Due to the highly scattered environment and absence of clear line of sight, we consider a frequency-selective Rayleigh fading channel for each coherence interval. It can be modelled as a linear time-varying filter $\mathbf{h}_{l,k}^t$ as follows (1).

$$\begin{aligned}\mathbf{H}_{l,k}^t &= \left[\mathbf{h}_{l,k}^0, \mathbf{h}_{l,k}^1, ..., \mathbf{h}_{l,k}^I\right] \in \mathbb{C}^{M\times I} \\ &= \left[\sqrt{\beta_{l,k}}\mathbf{g}_{l,k}^0, \sqrt{\beta_{l,k}}\mathbf{g}_{l,k}^1, ..., \sqrt{\beta_{l,k}}\mathbf{g}_{l,k}^I\right]\end{aligned} \tag{1}$$

with I and $\mathbf{g}_{l,k,n}^i \sim \mathcal{CN}(\mathbf{0}, \mathbf{I}_M)$ the number and the magnitude of time pulses respectively. The large-scale fading coefficient $\beta_{l,k}$ between AP l and UE k varies slowly along several coherence intervals and assumed to be known from a prior evaluation step. The channel estimates in the frequency domain are referred as $\hat{\mathbf{h}}_{l,k,n} \sim \mathcal{CN}(\mathbf{0}, \gamma_{l,k}\mathbf{I}_M)$ with $\gamma_{l,k} \triangleq \mathrm{E}\{|\left[\hat{h}_{l,k}\right] m|^2\}$ the mean-square of the estimate for any antenna m obtained through an uplink (UL) training phase using the minimum mean-squared error estimator given in [3]. This estimate is an approximation of the real channel coefficient such that $\mathbf{h}_{l,k,n} = \hat{\mathbf{h}}_{l,k,n} + \tilde{\mathbf{h}}_{l,k,n}$ with $\tilde{\mathbf{h}}_{l,k,n} \sim \mathcal{CN}(\mathbf{0}, \beta_{l,k} - \gamma_{l,k})\mathbf{I}_M)$ the estimation error caused by thermal noise and the HWI.

B. Downlink transmission

The time resource, corresponding to a TDD frame, is split between an UL training phase and a DL/UL data transmission. During this interval, a number of OFDM symbols N_c is transmitted over N_{sc} consecutive sub-carriers, and we denote $\tau_c = N_{sc}N_c$ the length in sample of the transmission. However, τ_p samples are reserved to be used as pilots for the training phase, leaving $\tau_d = \tau_c - \tau_p$ samples for the data transmission. The latter are split among the UL and the DL depending on a factor ξ where $0 < \xi < 1$.

We denote the data symbols transmitted through the n-th sub-carrier to the K UEs by $\mathbf{s}_n \in \mathbb{C}^{K\times 1}$. They are independent, have unit power such that $E\left\{\|\mathbf{s}_n\|^2\right\} = 1$ and are uncorrelated. For our OFDM system, we consider a guard band of size N_{GB} at both end of the spectrum where no power is allocated for the data transmit. The available sub-carriers are thus divided in two subsets: *(i)* Ξ, used for data transmission and *(ii)* its complementary Ξ^c, used for guard-band. Consequently, we have $\mathbf{s}_n = \mathbf{0}_{K\times 1}, \forall n \in \Xi^c$. For the sake of generality and for later benchmarking, we consider a non hardware-aware and a non-sequential processing scheme in this section. Hence, the data signal transmitted by AP l to all UEs is given by (2).

$$\mathbf{x}_{l,n} = \mathbf{W}_{l,n}\mathbf{P}_l\mathbf{s}_n, \tag{2}$$

with $\mathbf{W}_{l,n} \in \mathbb{C}^{M\times K}$ the precoding matrix for sub-carrier n at AP l and $\mathbf{P}_l \in \mathbb{C}^{K\times K}$ a diagonal matrix whose element $\sqrt{\eta_{l,k}}, k = 1, ..., K$ are the normalized DL transmit power which satisfies a per-AP constraint P_{max}^{DL}.

The CF-mMIMO normalized local partial zero-forcing (PZF) precoding scheme [3] is used. It exploits the differences in channel conditions among users to enhance overall system performance by locally splitting the users in a strong group S_l and a weak group W_l. A grouping threshold $v_l\%$ is defined which corresponding to the contribution to the sum of total channel gains from all UEs that are active within the coverage area of an AP l as follows (3).

$$\sum_{k=1}^{\tau_{S_l}} \frac{\bar{\beta}_{l,k}}{\sum_{t=1}^{K}\beta_{l,t}} \geq v_l\% \tag{3}$$

where $0 \leq \tau_{S_l} \leq \min(M, \tau_p+1)$ denotes the number of strong UEs selected by the l-th AP and $\{\bar{\beta}_{l,1}, ..., \bar{\beta}_{l,K}\}$ is the set of large-scale fading coefficients sorted in the descending order. The remaining UEs are put in the weak group W_l. Then, two different approaches are used to compute the precoder (4) : the FZF precoder is used $\forall k \in S_l$ and MRT $\forall k \in W_l$.

$$w_{l,n,k}^{\text{PZF}} = \begin{cases} \hat{\mathbf{H}}_{l,n}\left(\hat{\mathbf{H}}_{l,n}^H\hat{\mathbf{H}}_{l,n}\right)^{-1}\mathbf{e}_{i_k}\sqrt{(M-\tau_p)\theta_{l,k}}, & \forall k \in S_l \\ \hat{\mathbf{H}}_{l,n}\mathbf{e}_{i_k}/\sqrt{M\theta_{l,k}}, & \forall k \in W_l \end{cases} \tag{4}$$

with $\mathbf{e}_{i_k}$ the i-th column of $\mathbf{I}_{\tau_p}$ and $\theta_{l,k} = \gamma_{l,k}/c_{l,k}^2$ is obtained from the uplink training as detailed in [3].

III. QUANTIFIED DAC IMPAIRMENT MODEL

In this work, we consider a fixed-point quantization model where its effect $Q(x)$ is defined as $\mathrm{E}\{x|Q(x)\} = Q(x)$, which means the output of the DAC is equal to the mean of the interval containing the input value. Let x be a random complex variable with zero mean and Gaussian distribution. The signal

developed for the DL transmission in (2) is modulated into an OFDM signal and passed through an RF chain in order to feed the antenna. From the Bussgang theorem, it can be shown that the output of a nonlinear function is made of two terms [6] as (5).

$$y = Q(x) = K_0 x + d \tag{5}$$

with K_0 a complex scaling factor and d an uncorrelated additive noise. In the literature, realistic DAC component model are often omitted and empirical Bussgang coefficients are used to model the impairment [12], [13]. Here, we start from the definition of a signed output fixed-point DAC with a uniform quantizer. With such component, the amount of bit allocated to the integer and the fractional parts is known by design, and thus we can deduct all the intervals of quantization. Let i and f be the number of bit allocated to the integer and fractional resolution respectively. For simplicity, we assume that the dynamic range of the DAC is unitary and that our input signals are normalized to have a variance of one. The intervals q numbered from 0 to $2^i 2^f - 1$ can thus be deducted. Since the output of a DAC is the mean value of any quantization interval, we can find that for any input x, the DAC transfer function (6).

$$Q(x \in [q, q+1]) = \frac{1}{2}(Q_{int}(q) + Q_{int}(q+1)) \tag{6}$$

with $Q_{int}(q) = -2^{i-1} + q2^{-f}$ the boundary value delimiting the q-th interval from the preceding one. Thanks to this approach, we can deduct the Bussgang coefficients precisely from any integer/fractional pair of bits. Starting from the definition of the PDF for a normal distribution $p(x)$ with mean $\mu = 0$ and variance σ^2 : $p(x) = \frac{1}{\sqrt{2\pi\sigma^2}}/e^{-x/(2\sigma^2)}$, by performing a summation over all the existing intervals of the DAC, the primitive of all $Q(x)$ can be found. K_0 is derived from the correlated gain of the function as follows (7).

$$K_0 = \frac{\mathrm{E}\{Q(x)x\}}{(\mathrm{E}|x^2|)} = \frac{1}{\sigma^2}\int_{-\infty}^{+\infty} xQ(x)p(x)dx \tag{7}$$

After development, we find the scaling Bussang coefficient K_0 for any DAC resolution pair $(i|f)$ as given by (8).

$$K_0(i|f) = \frac{2^{-f}}{\sqrt{\pi 2\sigma^2}} \sum_{q=0}^{2if-1} \exp\left(\frac{Q_q}{2\sigma^2}\right) \tag{8}$$

The variance for the distortion noise σ_d^2 can be found by rearranging the terms $d = y - K_0 x$ of (5) as (9).

$$\sigma_d^2 = \left\{|Q(x)|^2\right\} - K_0\sigma^2 \tag{9}$$
$$\left\{|Q(x)|^2\right\} = \int_{-\infty}^{+\infty} Q(x)p(x)dx$$

After development, we find that the variance of the distortions noise under the specified distribution $p(x)$ is defined as in (10).

$$\sigma_d^2 = \frac{2^{-f}}{2} \sum_{q=0}^{(2^i 2^f)-1} \left(\mathrm{erf}\left(\frac{Q_q}{2\sigma^2}\right)\right) - K_0\sigma^2 \tag{10}$$

IV. Downlink achievable spectral efficiency

The performance in the band is evaluated at the user side as a data rate in the transmission band. The frequency-domain received signal at UE k and subcarrier n is given by (11).

$$\begin{aligned} y_{k,n} &= \sum_{l=1}^{L} \mathbf{h}_{l,k,n}^H \mathbf{z}_{l,n} + b_{k,n} \\ &= \sum_{l=1}^{L} \mathbf{h}_{l,k,n}^H \mathbf{K}_0 \mathbf{x}_{l,n} + \sum_{l=1}^{L} \mathbf{h}_{l,k,n}^H \mathbf{d}_{l,n} + b_{k,n}, \end{aligned} \tag{11}$$

where $\mathbf{z}_{l,n} \in \mathbb{C}^{M\times 1}$ denotes the frequency-domain amplified signal transmitted by AP l on sub-carrier n, $\mathbf{d}_{l,n} \in \mathbb{C}^{M\times 1}$ is the frequency-domain version of hardware-related noise, $\mathbf{K}_0$ is the $M \times M$ diagonal matrix whose elements are equal to K_0 and $b_{k,n} \sim \mathcal{CN}(0,1)$ is an i.i.d. Gaussian noise.

By plugging (2) in (11), $y_{k,n}$ can be expanded as

$$y_{k,n} = \sum_{l=1}^{L} \mathbf{h}_{l,k,n}^H \mathbf{K}_0 \mathbf{W}_{l,n} \mathbf{P}_l \mathbf{s}_n + \sum_{l=1}^{L} \mathbf{h}_{l,k,n}^H \mathbf{d}_{l,n} + b_{k,n} \tag{12}$$

$$= \underbrace{\sum_{l=1}^{L} \sqrt{\eta_{l,k}} \mathbf{h}_{l,k,n}^H \mathbf{K}_0 \mathbf{w}_{l,n,ik} s_{k,n}}_{\text{Desired signal}} + \underbrace{b_{k,n}}_{\text{Noise}} +$$

$$\underbrace{\sum_{l=1}^{L}\sum_{t\neq k}^{K} \sqrt{\eta_{l,t}} \mathbf{h}_{l,k,n}^H \mathbf{K}_0 \mathbf{w}_{l,n,i_t} s_{t,n}}_{\text{Multi-user interference}} + \underbrace{\sum_{l=1}^{L} \mathbf{h}_{l,k,n}^H \mathbf{d}_{l,n}}_{\text{HWI}} \tag{13}$$

with i_k and i_t the indices of the pilot sequences used by UE k and t respectively. It corresponds to the shared column vector designed for all UEs i_k and i_t in the precoder matrix in the presence of pilot contamination ($K > \tau_p$). The per-user spectral efficiency (SE) in the downlink can be computed as in (14).

$$\mathrm{SE}_k = \xi\left(1 - \frac{\tau_p}{\tau_c}\right)\log_2\left(1 + \mathrm{SINR}_{k,n}\right), \tag{14}$$

with the effective signal-to-interference-plus-noise ratio (SINR) of UE k at sub-carrier n, with a normalization by the noise power (15).

$$\mathrm{SINR}_{k,n} = \frac{|\mathrm{CP_{k,n}}|^2}{\mathrm{E}\left\{|\mathrm{PU_{k,n}}|^2\right\} + \sum_{t\neq k}^{K} \mathrm{E}\left\{|\mathrm{UI_{k,t,n}}|^2\right\} + \mathrm{E}\left\{|\mathrm{HWI_{k,n}}|^2\right\} + 1} \tag{15}$$

where $\mathrm{CP_{k,n}}$, $\mathrm{PU_{k,n}}$, $\mathrm{UI_{k,n}}$ and $\mathrm{HWI_{k,n}}$ are the coherent precoding, the precoding gain uncertainty, the multi-user interference and the hardware impairment respectively, and are given by (16, 17, 18, 19).

$$\mathrm{CP_{k,n}} = \sum_{l=1}^{L} \sqrt{\eta_{l,k}} \mathrm{E}\left\{\mathbf{h}_{l,k,n}^H \mathbf{K}_0 \mathbf{w}_{l,n,i_k}\right\} \tag{16}$$

$$\mathrm{PU_{k,n}} = \sum_{l=1}^{L} \left(\sqrt{\eta_{l,k}} \mathbf{h}_{l,k,n}^H \mathbf{K}_0 \mathbf{w}_{l,n,i_k} - \sqrt{\eta_{l,k}} \mathrm{E}\left\{\mathbf{h}_{l,k,n}^H \mathbf{K}_0 \mathbf{w}_{l,n,i_k}\right\}\right) \tag{17}$$

$$\mathrm{UI}_{\mathrm{k,t,n}} = \sum_{l=1}^{L} \sqrt{\eta_{l,k}} \mathbf{h}_{l,k,n}^{H} \mathbf{K}_0 \mathbf{w}_{l,n,i_t} \tag{18}$$

$$\mathrm{HWI}_{\mathrm{k,n}} = \sum_{l=1}^{L} \mathbf{h}_{l,k,n}^{H} \mathbf{d}_{l,n} \tag{19}$$

V. Out-of-band radiations

Frameworks for the assessment of OOB radiations exists in co-localized mMIMO [9]. They are mostly focused on the transmission pattern at the AP, where the contribution of the whole antenna array can be precisely determined, and thus, using channel reciprocity, it allows for an evaluation of its impact at the UEs. However, in our case, the antenna array is distributed among several, and widely spread, geographical points. Hence, we propose a new framework adapted to CF-mMIMO systems where the evaluation of the OOB radiations is done directly at the UE.

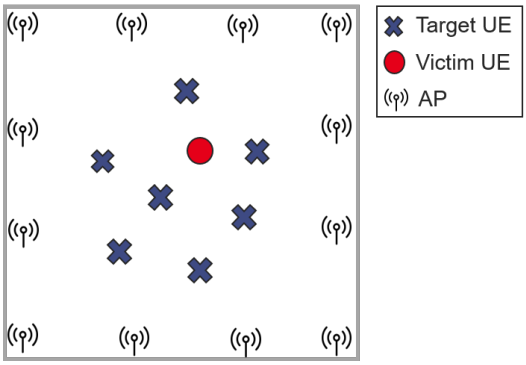

Fig. 1. A square simulation environment with a set of K target users focused by the APs and a victim UE placed among them.

We define two separate groups of users. On the one hand, we have the K target UEs, that are actively treated as part of the UL training and the DL precoding and data assignment sequences by the APs. On the other hand, a single victim UE which operates on an adjacent channel is placed among the target UEs in the simulation environment, as depicted on Fig. 1. While not being included in the precoder design, the victim receives a fraction of the power emitted toward the target UEs which varies according to their relative position to the targets and the chosen precoder scheme and system parameters. While the in-band power is not detrimental for the victims, the non-linearities of the signal brought by the DAC cause spectral regrowth on the adjacent channels. With the assumption that the victims are operating on adjacent channels, this unintended power leads to a degradation of their communication in the form of parasitic signal. The signal received by the victim UE on all N sub-carrier can be found with equation (11) and using the real channel coefficient $\mathbf{h}_{l,k,n}^{H}$ between the victim UE k and AP l, the contributions of the APs being unchanged compared to the formula in (11). Then, simulation data are gathered across several channel realisation and UL training/DL transmit sequences for all sub-carrier so that a power spectral density can be obtain using the received signal in the frequency domain $y_{k,n}$. Since a spectrum span of equivalent width as the active band is allocated for the guard band on both side of the spectrum such that $N_{GB} = N/3$, the OOB leakage can be observed and quantified by simulation. We define the received OOB power $P_{OOBr}(k)$ metric at UE k as the sum of all sub-carriers contribution over their frequency span in the left adjacent channel (guard band) (20).

$$P_{OOBr}(k) = \sum_{n=0}^{N_{GB}} (|y_{k,n}|^2) B_n \tag{20}$$

with $B_n = B/N$ the spacing in Hz between sub-carriers (B being the bandwidth) and $|y_{k,n}|^2$ the power spectral density at each sub-carrier at UE k. Note that this metric is an overestimation of the real received OOB power as we assume the sub-carriers have the same power along all their width due to the discrete computation on each sub-carrier in (11).

VI. Simulation and experimental results

A. Simulation parameters

TABLE I
Simulation settings.

Description	Value	Description	Value
D (simulation area)	$60 \times 60m$	UE distribution	random
M	8	τ_p, K	7
L	48	AP/UE antenna height	10/1.5 m
Noise power	-93 dBm	P_{max}^{DL}	1000 mW
UL transmit power	100 mW	τ_c	168
ξ	0.5	σ_{sh}	4 dB
Carrier frequency	3.5 GHz	B	20 MHz
N_{snap}	500	R	25

We consider a scenario with a serial fronthaul network wrapped around a 60 by 60 meter square environment as in Fig. 1. The large-scale fading coefficients $\beta_{l,k}$ are modeled as in [3] by (21).

$$\beta_{l,k} = \mathrm{PL}_{l,k}.10^{\frac{\sigma_{sh} z_{l,k}}{10}}, \tag{21}$$

where $\mathrm{PL}_{l,k}$ denotes the path-loss and $10^{\frac{\sigma_{sh} z_{l,k}}{10}}$ models log-normal shadow fading with standard deviation σ_{sh} and $z_{l,k} \sim \mathcal{N}(0,1)$. Note that, in this investigation, we consider the 3GPP path-loss model, which is given by equation (22) when assuming a sub-6 GHz carrier frequency [3].

$$\mathrm{PL}_{l,k}\,[\mathrm{dB}] = -22.7 - 36.7\log_{10}\left(\frac{d_{l,k}}{1\ m}\right) - 26\log_{10}\left(\frac{f_c}{1\ \mathrm{GHz}}\right), \tag{22}$$

where f_c is the carrier frequency and $d_{l,k}$ denotes the distance between the l-th AP and the k-th UE including AP and UE's heights. The simulation settings are reported in Table I except otherwise stated. The UL and noise power are used for the UL training described in [3], and a number R of independent channel realisations and transmission sequences are performed over the N_{snap} random environment generation before performance evaluation. For the out-of-band simulations, they are 150 canal realisations drawn before establishing the power density function for a snapshot. A cyclic prefix composing 7% of the symbol's length is also added at the end of each symbol in order to get a pseudo-circular convolution

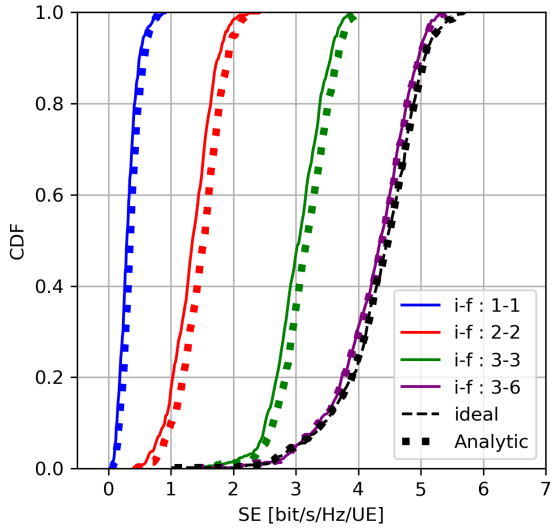

Fig. 2. CDF of the in-band SE for various integer (i) - fractional (f) resolution pairs

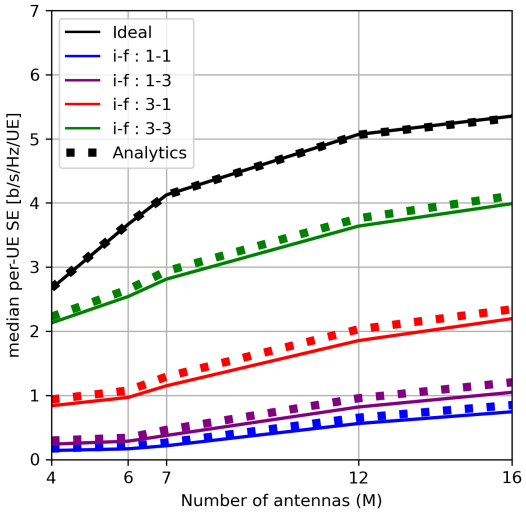

Fig. 3. Mediane SE against number of antennas

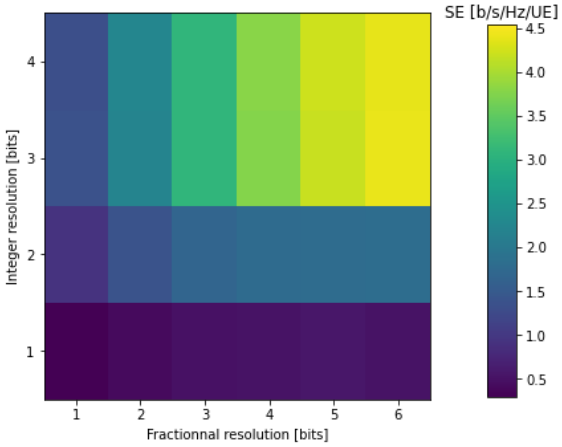

Fig. 4. Mediane per-UE SE against resolution of the DAC

when computing the signal receive at an UE. The 128 sub-carriers in the band and a guard band of size 128 on the two sides. The sub-carrier at central frequency (0 Hz or DC) have been filtered prior to generating the PDF and OOB radiation figures.

B. Results

First, we focus on the in-band performance of the system. The cumulative density functions (CDF) for various integer/fractional DAC resolution pairs are shown in Fig. 2. It appears clear that at the lowest resolutions, the performance degradation is extreme with a near-zero SE for at least 50% of the snapshots for i|f = 1|1. It also appears that the analytic results are a few percent off compared to the simulation (obtained from (15)) for the medium levels of HWI. It may arises from an extrapolation of the impairment level from only one sub-carrier in our simulation whereas the analytic depicts the expected value for any sub-carrier. However, it is small enough so that the performance evaluation gives a good estimate of the impact of DAC impairment on the system.

On Fig. 3, the median SE against number of antennas of the system is given. First of all, it is worth mentioning that, thanks to the PZF precoder, the system operates when the condition $M - \tau_p \geq 0$ is not satisfied ($M = 4, 6$) as opposed to the FZF precoder often used in the literature. The achievable SE increase steadily up to $M = \tau_p = 7$ in the ideal case, thanks to increased coherent precoder gain. However, this behavior is not found for the low-resolution DAC as each added antenna comes with its own strong distortions, which adds a comparable increase in magnitude of the HWI compared to the array gain.

On Fig. 4, the achievable median SE against the DAC resolution is given, which shows that the integer resolution is a limit factor until 3 bits, at which points the normalized input signal distribution with variance $\sigma^2 = 1$ and zero mean is nearly completely within the boundary values of the first and last quantization intervals. Then, each additional fractional bit brings the the achievable SE closer to the ideal, which is almost reached for $i|f = 3|6$ as seen on Fig 2.

For the out-of-band analysis, we are interested in assessing the damages caused on the adjacent channel at the victim. On Fig. 5, the power spectral density received at the position of a random target and a random victim UEs obtained through averaging over 500 snapshots are shown. The PSD are normalized by the max power in dB in the band of the target, which correspond to the expected useful signal power with the system parameters of the simulation. We see that with an ideal DAC, the victim receives less than -50 dB of power on each sub-carrier on the adjacent channel, which is sufficiently low to not disturb its intended communication. With the lowest resolution profile (1 integer and 1 fractional bit), this power is increases to -36 dB per sub-carrier in the out-of-band region which again is negligible. This result is similar to the one obtained in co-localized large antenna array, where the high directivity prevents victim UEs to be contaminated by neighbouring communications [9]. We can also see that the target receives less power in the band when the resolution is

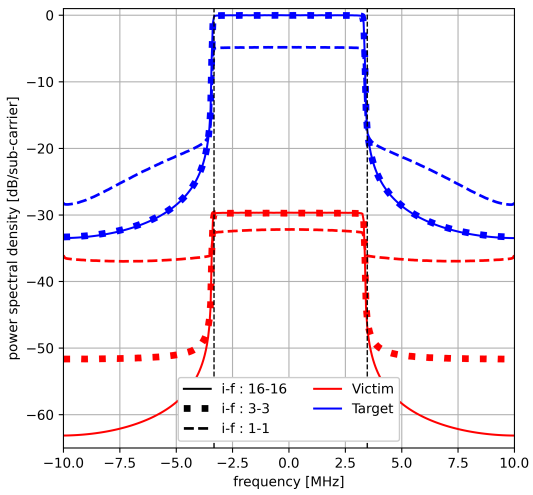

Fig. 5. Mean power spectral density acquired at the position of the target and the victim UE for different integer (i) - fractional (f) resolution pairs. The PSD is normalized by the maximum received power at the target.

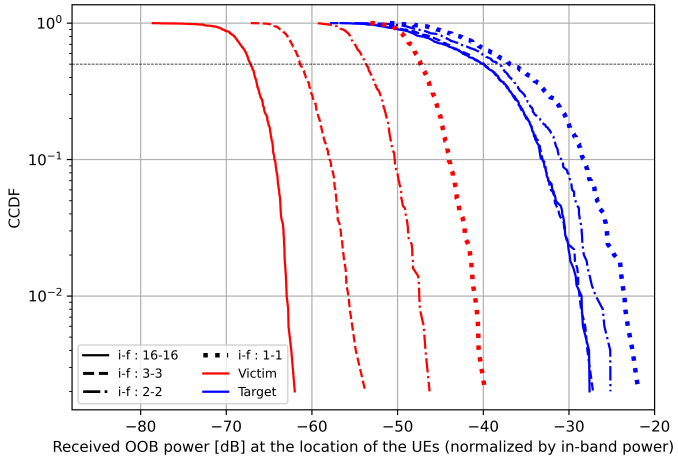

Fig. 6. CCDF of the ajdacent channel power at the position of the target and the victim UE for different integer [i]/fractionnal [f] DAC resolutions

low, with around -5 dB compared to the ideal. This is due to the integer range not covering the amplitude of the input signal distribution, thus clipping the signal into less power-heavy levels. Meanwhile, on Fig. 6, the CCDF of the out-of-band power P_{OOBRr} for each snapshot is shown using a normalization by the the cumulated power in-band at the target. We see that in the worst case, with the lowest resolution, the total out-of-band power at the target is - 23 dB below its in-band power, while the victim receives a 100 times lesser amount of power. It can also be seen that the tail of the CCDF at the target and at the victim, as well as the ideal case compared to the low resolution, is way wider. This is likely due to the dominance of random multipath-induced fading in the distribution of the OOB power brought by the directivity of the transmission. Meanwhile, the OOB power caused by the HWI has a small variance since each antenna are affected by a statistically limited variety of distortions over all sub-carriers.

Conclusion

In this work, the impact of a fixed-point DAC with a fixed input distribution have been evaluated for a CF-mMIMO OFDM based system. Thanks to the known behavior and quantizer interval of such component, analytic closed form expressions to obtain the Bussgang coefficients have been derived. Results show that a low DAC resolution severely impacts the performance of the system in the band. Moreover, we developed a CF-mMIMO-adapted framework to assess the impact of out-of-band radiation. Results have shown that victim UE adjacent to the target cluster should not be significantly impaired if they operate on an adjacent channel. Further studies need to be carried to compare precoding scheme where the orthogonalisation of exploited channels is less intense such as with MRT precoder. Then, a HWI cancelation precoding scheme could be developed for fixed-point DAC based system enhancement.

Acknowledgment

This work was supported in part by the ANR under the France 2030 program, grant "NF-PERSEUS: ANR-22-PEFT-0004" and by the framework of the ALEX6 Project receiving fund by the French CARNOT-ANR under Carnot-SCIENCE-ALEX6.

References

[1] A. Lozano, R. W. Heath, and J. G. Andrews, "Fundamental Limits of Cooperation," *IEEE Transactions on Information Theory*, vol. 59, no. 9, pp. 5213–5226, 2013.

[2] S. Chen, J. Zhang, J. Zhang, E. Björnson, and b. ai, "A survey on user-centric cell-free massive MIMO systems," *Digital Communications and Networks*, vol. 8, 12 2021.

[3] G. Interdonato, M. Karlsson, E. Björnson, and E. G. Larsson, "Local Partial Zero-Forcing Precoding for Cell-Free Massive MIMO," *IEEE Transactions on Wireless Communications*, vol. 19, no. 7, pp. 4758–4774, 2020.

[4] E. Björnson and L. Sanguinetti, "Scalable Cell-Free Massive MIMO Systems," *IEEE Transactions on Communications*, vol. 68, no. 7, pp. 4247–4261, 2020.

[5] J. Zhang, Y. Wei, E. Björnson, Y. Han, and S. Jin, "Performance Analysis and Power Control of Cell-Free Massive MIMO Systems With Hardware Impairments," *IEEE Access*, vol. 6, pp. 55 302–55 314, 2018.

[6] O. T. Demir and E. Bjornson, "The Bussgang Decomposition of Nonlinear Systems: Basic Theory and MIMO Extensions [Lecture Notes]," *IEEE Signal Processing Magazine*, vol. 38, no. 1, pp. 131–136, 2021.

[7] Y. Zhang, Y. Cheng, M. Zhou, L. Yang, and H. Zhu, "Analysis of Uplink Cell-Free Massive MIMO System With Mixed-ADC/DAC Receiver," *IEEE Systems Journal*, vol. 15, no. 4, pp. 5162–5173, 2021.

[8] M. Zhou, Y. Zhang, X. Qiao, M. Xie, L. Yang, and H. Zhu, "Multigroup multicast downlink cell-free massive mimo systems with multiantenna users and low-resolution adcs/dacs," *IEEE Systems Journal*, vol. 16, no. 3, pp. 3578–3589, 2022.

[9] C. Mollen, E. G. Larsson, U. Gustavsson, T. Eriksson, and R. W. Heath, "Out-of-band radiation from large antenna arrays," *IEEE Communications Magazine*, vol. 56, no. 4, pp. 196–203, 2018.

[10] Z. H. Perić and M. R. Dinčić, "Optimization of the 24-bit fixed-point format for the laplacian source," *Mathematics*, vol. 11, no. 3, 2023.

[11] R. Zayani, J.-B. Doré, B. Miscopein, and D. Demmer, "Local PAPR-Aware Precoding for Energy-Efficient Cell-Free Massive MIMO-OFDM Systems," *IEEE Transactions on Green Communications and Networking*, vol. 7, no. 3, pp. 1267–1284, 2023.

[12] S. Dey and R. Budhiraja, "FD Cell-Free Massive MIMO Systems With Downlink Pilots: Analysis and Optimization," *IEEE Transactions on Communications*, vol. 70, no. 11, pp. 7591–7608, 2022.

[13] M. Zhou, Y. Zhang, X. Qiao, W. Tan, and L. Yang, "Analysis and optimization for downlink cell-free massive mimo system with mixed dacs," *Sensors*, vol. 21, no. 8, 2021. [Online]. Available: https://www.mdpi.com/1424-8220/21/8/2624